

# Synergist Flame Retarding Effect of Ultrafine Zinc Borate on LDPE/IFR System

Zhiping Wu,<sup>1,2</sup> Wanyin Shu,<sup>1</sup> Yunchu Hu<sup>2</sup>

<sup>1</sup>School of Chemistry and Chemical Engineering, Central South University, Changsha 410083, China

<sup>2</sup>School of Industry, Central South University of Forestry and Technology, Changsha 410004, China

Received 20 May 2006; accepted 28 September 2006

DOI 10.1002/app.25575

Published online in Wiley InterScience (www.interscience.wiley.com).

**ABSTRACT:** The flame retardancy of low-density polyethylene (LDPE) treated with complex flame retardant composed of ultrafine zinc borate (UZB) and intumescent flame retardant (IFR) have been investigated by limited oxygen index (LOI), UL-94 test, thermogravimetric analysis (TGA), cone calorimeter test, scanning electron micrograph (SEM), energy-dispersive spectrometer (EDS), and X-ray diffraction (XRD). The results of LOI and UL-94 test indicate the desired flame retardancy of LDPE is obtained when the mass ratio of UZB to IFR is 4.2 : 25.8 and the complex flame retardant mass content is 30% (based on LDPE). The results of cone calorimeter show that heat release rate (HRR) peak, total heat release (THR), and mass loss of LDPE/IFR/UZB decrease substantially when compared with those of LDPE/IFR. TGA results show that the residue of

LDPE/IFR/UZB increases obviously than that of LDPE/IFR when the temperature is above 600°C. SEM indicates the quality of char forming of LDPE/IFR/UZB is superior to that of LDPE/IFR. The results of EDS and XRD indicate that boron orthophosphate (BPO<sub>4</sub>) and zinc-contained compounds are formed in the residual char and these substances may play an important role in stabilizing the intumescent char structure and decrease the degradation speed substantially when subjected to high temperature. © 2006 Wiley Periodicals, Inc. *J Appl Polym Sci* 103: 3667–3674, 2007

**Key words:** ultrafine zinc borate; intumescent flame retardant; complex flame retardant; low-density polyethylene; flame retardancy

## INTRODUCTION

Low-density polyethylene (LDPE) is widely used in many fields owing to its good electrical insulation, low cost, and easy processability<sup>1</sup>; however, easy combustibility (LOI < 18) and melt dripping limit its applications. It is essential to improve the flame retardancy of LDPE to reduce the hazard of fire.<sup>2</sup> The traditional method to improve the flame retardancy of LDPE is to introduce halogen-contained flame retardant to polymer matrix. However, LDPE treated with halogen-contained flame retardant will produce harmful and corrosive hydrogen halide and density smoke owing to the synergist of antimony oxide. The research in halogen-free flame retardant has become a hot issue. The effective halogen-free flame retardants are intumescent flame retardant (IFR) and inorganic flame retardant.<sup>3,4</sup> The flame retarding behavior of IFR for polymer is the formation of an expanded charring layer at the burning surface, so that oxygen and heat transfer toward the undecomposed bulk is prevented.

IFR formulation, first used in the painting industry, has been applied to the fire stabilization of polymeric materials.<sup>5</sup> The typical formulation of IFR constitutes: carbonific agent, carbonific catalyst, and blowing agent. Although most research in IFR focus on polypropylene,<sup>6–10</sup> the research in IFR applied to polyethylene has attracted some peoples' concern.<sup>11–13</sup> Zinc borate is an effective inorganic flame retardant and possesses the characteristics of flame retarding, smoke suppression, extinguish dripping, promoting charring, etc.<sup>14,15</sup> Bourbigot et al.<sup>16</sup> studied the fire and smoke behaviors of EVA24-ATH/FBZB and EVA24-Mg(OH)<sub>2</sub>/FB415 by limited oxygen index (LOI), cone calorimeter, and thermogravimetric analysis (TGA). Solid-state NMR was employed to study the carbon in the residues collected from the cone calorimeter experiments. It is proposed that zinc borate aids in developing a more vitreous protective residual layer, which reduces the combustion rate. Carpentier et al.<sup>17</sup> studied the synergist effect of zinc borate (FB415) on EVA8 filled with magnesium hydroxide (MH), by LOI, cone calorimeter, and TGA. Solid-state NMR was employed to study the carbon in the residues collected after thermal treatment. It is suggested that zinc borate slows the degradation of the polymer and creates a vitreous protective residual layer, which could act as a physical barrier and a glassy cage for polyethylene chains. Kim<sup>18</sup> reported that zinc borate and talc can effectively increase the flame retardance of PE filled

Correspondence to: Z. Wu (wuzhiping02@163.com).

Contract grant sponsor: Nation Natural Science Foundation of China; contract grant number: 30471358.

Contract grant sponsor: Zhuzhou City Scientific Research Funds; contract grant number: 20040603.

*Journal of Applied Polymer Science*, Vol. 103, 3667–3674 (2007)  
© 2006 Wiley Periodicals, Inc.

with MH, and the synergistic effect was observed when zinc borate and talc were incorporated together. Xie et al.<sup>19</sup> studied the synergist effect of expandable graphite (EG) and zinc borate employed by LOI, UL-94 test, and cone calorimeter test. Bourbigot and coworkers<sup>20,21</sup> reported the potential application of zinc borate in PP-based IFR system. The diameter of general zinc borate is 4–7  $\mu\text{m}$ ; reducing the particles diameter is essential to improve the compatibility between inorganic particles and polymer matrix.<sup>22,23</sup> In a previous work,<sup>24</sup> we studied the preparation and characteristics of ultrafine zinc borate (UZB) and the effect of the IFR composition on the flame retardancy of LDPE. The study of mechanical properties improvement of UZB on LDPE/IFR has been described elsewhere.<sup>25</sup> This work is devoted mainly to study the synergist flame retarding effect of UZB on LDPE/IFR based on LOI, UL-94 test, and cone calorimeter. TG-DTA, SEM, energy-dispersive spectrometer (EDS), and X-ray diffraction (XRD) are also employed to further understand the flame retarding mechanism.

## EXPERIMENTAL

### Materials

Low-density polyethylene (LDPE; commercial grade) was from Beijing Yanshan Petrochemical 1F7B, ammonium polyphosphate (APP) was supplied by GD Chem. of Zhejiang Longyou, DP > 1500, pentaerythritol (PER) was chemical agent from Shanghai Chemical Agent Station, IFR (blends of APP and PER, the mass ratio of APP to PER is 3 : 2), ultrafine zinc borate ( $2\text{ZnO} \cdot 3\text{B}_2\text{O}_3 \cdot 3.5\text{H}_2\text{O}$ ) was prepared in our laboratories (average diameter 73 nm and 90% particle diameter below 100 nm), complex flame retardant (blends of UZB and IFR).

### Preparation

Complex flame retardant was prepared by mixing UZB and IFR according to designed mass ratio; IFR or complex flame retardant were mixed with LDPE in a two-roll mixer (SK-160B, Shanghai, China) at 120–130°C for 20 min. The mixed samples were pressed into 3-mm sheet in a vulcanizing press machine (DLB500  $\times$  500, Wuxi, China) at 130–140°C, and samples of various size were obtained according to the testing standard.

### Measurement

LOI was performed according to ISO4589 in oxygen index tester (JF-3, Nanjin, China); the sample was  $130 \times 6.5 \times 3.0 \text{ mm}^3$ .

UL-94 test was performed according to GB4609-84 in vertical burning tester (CZF-2, Nanjin, China); the sample was  $130 \times 13 \times 3.0 \text{ mm}^3$ .

Cone calorimetry test was performed using a Stanton Redcroft cone calorimeter following the procedure defined in ASTM E 1354. The samples were put in horizontal orientation at an incident flux of 35  $\text{kW}/\text{m}^2$ . Specimen size is  $100 \times 100 \times 3 \text{ mm}^3$ , and the samples exposed to the incident irradiance is 88.4  $\text{cm}^2$ .

A differential thermal analytical balance (HCT-2, Beijing, China) was used for TGA and DTA. All measurements were conducted under a static air, and the weight of sample was  $7.5 \pm 0.1 \text{ mg}$ , heating rate was 10°C/min, and the test temperature range was from ambient to 800°C, and the pan used was ceramic pan.

The scanning electron micrographs of residual samples were observed by a JSM-6360LV scanning electron microscopy (JEOL JSM-6360LV scanning electron microanalyzer). The residual samples obtained from LDPE/IFR and LDPE/IFR/UZB heated at 550°C for 30 min were previously coated with a conductive gold layer.

EDS of residual samples were performed by energy-dispersive spectroscopy X-ray microanalyzer (EDAX, USA).

XRD of residual samples were performed by X-ray diffractory instrument (D/Max2500PC, Japan) with  $\text{Cu K}\alpha_1 = 0.154056 \text{ nm}$  radiation.

## RESULTS AND DISCUSSION

### LOI and UL-94 test

Testing results of flammability of untreated LDPE and LDPE treated with different mass ratios of UZB to IFR are listed in Table I. The data presented indicate that LOI value increase substantially when 30% IFR is introduced into LDPE and LOI is 24.5 (PE2). LOI value can further increase when part of IFR is substituted by UZB, the LOI value is 26.2, and the UL-94 can reach V0 rating when the mass ratio of UZB to IFR is 4.2 : 25.8 (PE7), and the content of complex flame retardant is 30% (based on LDPE), which indicates that the synergist flame retardancy effect exist between UZB and IFR in LDPE. But the LOI value will decrease when the mass ratio of UZB to IFR is greater than 4.2 : 25.8, which may be explained when the content of UZB below the critical value, the dispersibility of UZB particles is good, and the LOI value increases with the content of UZB increase.<sup>26,27</sup> However, the particles of UZB will agglomerate and the dispersibility will deteriorate when the content of UZB is above the critical value. In addition, the decreasing of expanded volume of LDPE/IFR/UZB can be visualized during the LOI and UL 94 test experiment when the mass ratio of UZB to IFR is greater than 4.2 : 25.8. This may be attributed to the content

TABLE I  
LOI Values and UL-94 Test Results of Untreated and Treated LDPE Formulations

Sample	LDPE (g)	Superfine zinc borate (g)	IFR <sup>a</sup> (g)	LOI (%)	UL-94 rating
PE1	100	0	0	17.8	burning
PE2	100	0	30	24.5	V-1
PE3	100	0.8	29.2	24.9	V-1
PE4	100	1.3	28.7	25.5	V-1
PE5	100	2.5	27.5	25.7	V-1
PE6	100	3.3	26.7	26.0	V-1
PE7	100	4.2	25.8	26.2	V-0
PE8	100	5.5	24.5	25.4	V-1
PE9	100	6.7	23.3	25.0	V-1

<sup>a</sup> The composition of IFR is APP/PER = 3 : 2 (mass ratio).

of IFR, which is too low, when the mass ratio of UZB to IFR is greater than 4.2 : 25.8, and the expanded effect of IFR is reduced obviously. These two factors will affect its flame retardancy. So the optimum mass ratio of UZB to IFR is 4.2 : 25.8.

#### Cone calorimeter test

LDPE, LDPE/IFR, and LDPE/IFR/UZB are represented by the samples of PE1, PE2, and PE7, respectively. They are chosen to undertake further studies because they represented the typical composition of untreated LDPE, LDPE treated with IFR, and LDPE treated with complex flame retardant. Cone calorimeter test is a small-scale test, but it has good correlation with real fire disaster, compared with LOI test; the data obtained from cone calorimeter can provide plentiful information on fire.<sup>28</sup> The heat release rate (HRR) and total heat release (THR) are presented in Figures 1 and 2. HRR is recognized to be the most important parameter to measure the developing and spreading of fire; it provides an indication of the likely size of the fire.<sup>29</sup> The results of Figure 1 shows that the HRR peak of LDPE/IFR/UZB is the smallest (131 kW/m<sup>2</sup>). The HRR peak decreased with 72% when compared with that of the LDPE (466 kW/m<sup>2</sup>), and decreased with 46% when compared with that of LDPE/IFR (244 kW/m<sup>2</sup>).

It is interesting to observe that the shape of untreated LDPE and treated LDPE (LDPE/IFR, LDPE/IFR/UZB) are distinct: untreated LDPE has a single peak at 155 s, and treated LDPE have double peaks. The first peak of the double peaks can be attributed to heat release of the combustible gas burning; the combustible gas is produced by the degradation of treated LDPE when they are subjected to high temperature, and at the same time, the charring layer is formed through etherification, dehydration, expansion, and crosslinking process. The charring layer on burning surface can prevent the further degradation of inner LDPE. So the amount of combustible gas decreases and the combustible heat decreases accordingly. The

valley appears behind the first peak of HRR. The second peak of the double peaks can be attributed to the heat release of charring layer oxidation. Although the HRR is lower in the valley than in the peak, the THR is still increasing and the temperature increase accordingly. The charring layer will oxidize under high temperature and heat release is inevitable. So the second peak of HRR appears behind the valley. There is no charring layer on the burning surface of untreated LDPE, and so the degradation rate of LDPE is fast and produces large amount of combustible gas, and the combustion cannot diminish until most of LDPE lost. The valley between double peaks cannot appear, and so there is only a single peak in the untreated LDPE combustible process. The phenomenon is corresponding to the shape of TGA curves. There is a plateau between the first mass loss stage and the second mass loss stage on the TG curves of treated LDPE; however, there is no plateau on the TG curve of untreated LDPE.

Another interesting aspect is that the beginning ignition time of treated LDPE (LDPE/IFR, LDPE/IFR/UZB) is shorter than that of untreated LDPE, and is corresponding to the lower temperature of initial mass

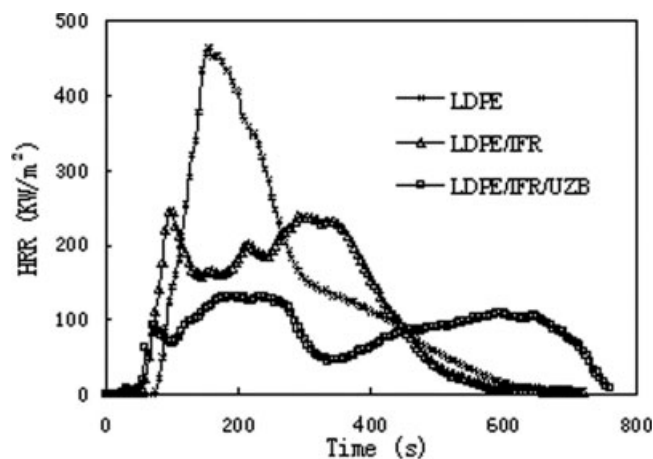


Figure 1 HRR curves of untreated LDPE and treated LDPE.

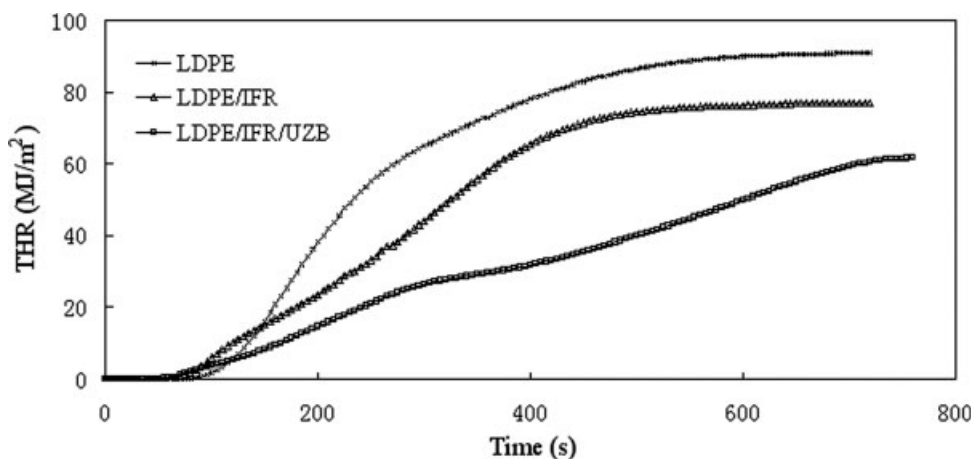


Figure 2 THR curves of untreated LDPE and treated LDPE.

loss of TG curves of the treated LDPE. This can be explained by the catalysis effect of IFR or complex flame retardant on the degradation of LDPE. So the treated LDPE produces combustible gas earlier and the beginning ignition time is shorter than that of untreated LDPE.

Although both LDPE/IFR and LDPE/IFR/UZB have double peaks, there exist differences in their HRR curves. The second HRR peak ( $238 \text{ kW/m}^2$ ) is nearly equal to the first HRR peak ( $244 \text{ kW/m}^2$ ) of LDPE/IFR; however, the second HRR peak ( $108 \text{ kW/m}^2$ ) is lower than the first HRR peak ( $131 \text{ kW/m}^2$ ) of LDPE/IFR/UZB. The time of double peak appearance of the latter is later than the former, and it can be explained that the charring layer of LDPE/IFR/UZB is superior to that of LDPE/IFR and can endure more time at the same temperature. It can be seen from Figure 2 that the order of total THR is: untreated LDPE ( $91.05 \text{ MJ/m}^2$ ) > LDPE/IFR ( $77.09 \text{ MJ/m}^2$ ) > LDPE/IFR/UZB ( $61.65 \text{ MJ/m}^2$ ), and it is the positive evidence to demonstrate the good synergist effect of UZB on LDPE/IFR system.

Mass curves of LDPE, LDPE/IFR, and LDPE/IFR/UZB are presented in Figure 3. It can be seen from Figure 3 that the mass loss of LDPE/IFR/UZB is the smallest (55.4%) when compared with that of the LDPE/IFR (70.3%) and that of LDPE (94.3%) during the whole combustion process. So the synergist flame retarding effect of UZB on LDPE/IFR results from the protection of high quality charring layer. This protection leads to increase in the residue and decrease in the combustible gas during the combustion process, and so the HRR and THR decreases accordingly.

#### Thermogravimetric and differential thermal analysis

Thermal analytical techniques [thermogravimetric and differential thermal analysis (TGA-DTA)] are effective

methods to investigate the flame retarding materials and flame retarding mechanism.<sup>30</sup> The results of TGA and DTA are presented in Figures 4 and 5, respectively. It can be seen from Figure 4 that the temperature of initial mass loss of LDPE/IFR is lower than that of untreated LDPE; the temperature of 1% mass loss is  $225$  and  $250^\circ\text{C}$ , respectively. However, the mass loss rate of untreated LDPE is obviously higher than that of LDPE/IFR when the temperature is above  $310^\circ\text{C}$ , and the temperature and mass loss rate corresponding to the maximum mass loss rate of untreated LDPE is  $423^\circ\text{C}$  and  $1.20\% \text{ }^\circ\text{C}^{-1}$  when compared with  $470^\circ\text{C}$  and  $1.05\% \text{ }^\circ\text{C}^{-1}$  of LDPE/IFR, respectively. It implied that IFR could decrease the initial degradation temperature and promote charring earlier, enhance the temperature of maximum mass loss rate, broaden the range of mass loss, and decrease the maximum mass loss rate. The temperature of 1% mass loss of LDPE/IFR/UZB is  $244^\circ\text{C}$ , and this implied that the heat stability was improved when UZB is incorporated into

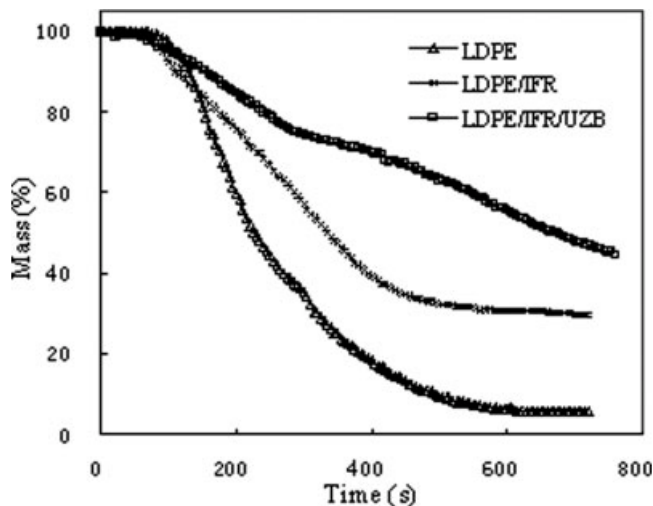


Figure 3 Mass curves of untreated LDPE and treated LDPE.



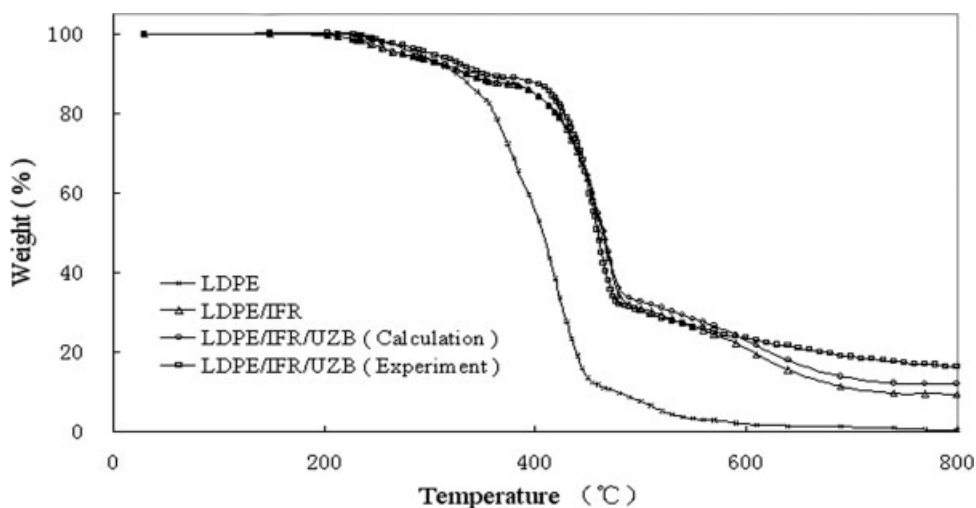


Figure 4 TGA curves of untreated LDPE and treated LDPE.

LDPE/IFR system. The TG curves of LDPE/IFR and LDPE/IFR/UZB are almost overlap when temperature is below 540°C. However, the mass loss rate of the latter is obviously lower than that of the former when the temperature is above 540°C, the maximum mass loss rate of the latter is  $0.09\% \text{ } ^\circ\text{C}^{-1}$  and lower than the former ( $0.14\% \text{ } ^\circ\text{C}^{-1}$ ) during this stage (540–800°C). The residue of the latter at 800°C is 16.4% when compared with 9.44% of the former. This can be attributed to the UZB that can protect char and decrease its oxidization speed at high temperature.

The shape of the TG curves is interesting to explain the flame retardancy of untreated and treated LDPE. The TG curve of LDPE can divide two mass loss stages: the first stage is the major mass loss stage (250–465°C,  $-\Delta W \approx 90\%$ ). Mass loss is fast and a large amount of combustible gas is produced, and this leads to huge exothermic peak that appears in the DTA curve of LDPE. And, the second stage is attributed to the little residue that continues oxidization with the increase in temperature, but the exothermic peak is small. The TG curves of LDPE/IFR can divide three mass loss stages: the first stage is 225–355°C and  $-\Delta W \approx 12\%$ , a plateau (355–380°C) appears after the first mass loss stage. It can be explained that the charring layer on the surface prevents the inner LDPE degradation, so the mass loss is approached to zero. The protective function of charring layer is diminished with the increase in temperature, and the second mass loss appears. The second mass loss stage is the major mass stage (380–480°C,  $-\Delta W \approx 56\%$ ), where oxidation of charring layer and the degradation of inner LDPE both occur in this stage under medium temperature. The third mass loss stage occurs at 480–800°C and  $-\Delta W \approx 23\%$ , and the mass loss can be attributed to the oxidation of char under high temperature. The TG curves of LDPE/IFR/UZB can also divide three mass loss stages: the first stage is 240–350°C and  $-\Delta W \approx 10\%$ ,

and a plateau (350–405°C) also appears and is more horizontal and broad when compared with the plateau of TG curves of LDPE/IFR. This indicates that the charring layer of LDPE/IFR/UZB has the better protection to inner LDPE when compared with that of LDPE/IFR, and this leads to the mass preserves constant range 350–405°C. The protection function of charring layer is also affected with the increase in temperature, and the second mass loss appears. The second mass loss stage is the major mass loss stage (405–490°C,  $-\Delta W \approx 56\%$ ). Oxidation of charring layer and the degradation of inner LDPE both occur in this stage under relative high temperature. The third mass loss stage occurs at 490–800°C and  $-\Delta W \approx 17\%$ ; the mass loss can be attributed to the oxidation of char under high temperature. The mass loss of the third stage of LDPE/IFR/UZB is smaller than that of

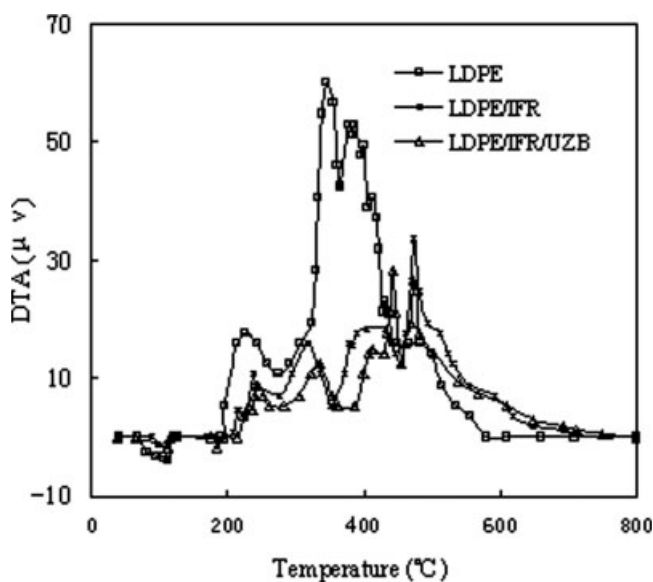
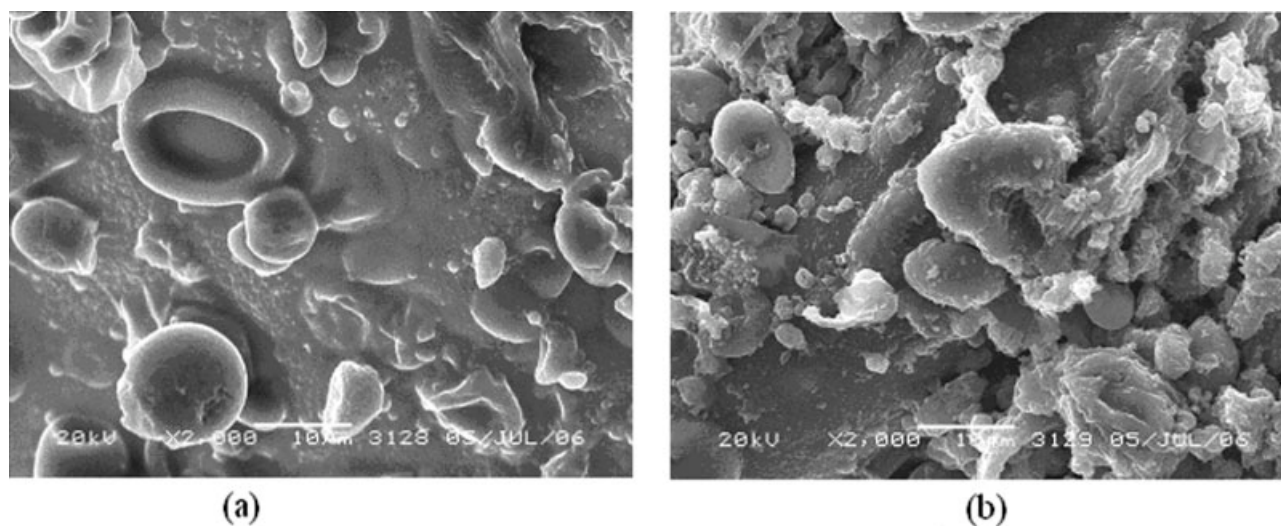


Figure 5 DTA curves of untreated LDPE and treated LDPE.



**Figure 6** Scanning electron micrograph of residual samples of (a) LDPE/IFR and (b) LDPE/IFR/UZB heated at 550°C for 30 min.

LDPE/IFR, and this can be explained that the resistivity to high temperature of char of the former is higher than that of the latter.

The TG curves of the theoretical (calculation) and experimental are employed to further understand the synergist effect of UZB on the LDPE/IFR system in Figure 4. LDPE/IFR/UZB (calculation) =  $(1 - \alpha) \times \text{TG}(\text{LDPE/IFR}) + \alpha \times \text{TG}(\text{UZB})$ , where  $\alpha$  represents the mass percent of UZB in the LDPE/IFR/UZB ( $\alpha = \frac{42}{130} \times 100\%$ ). It can be seen that the experimental curve is above the theory curve when the temperature is above 600°C. The residue of 800°C of the former and the latter is 16.4 and 11.1%, respectively. According to the formula of Van Krevelen:  $\text{LOI} = (17.5 + 0.4\text{CR})/100$ . CR is the residue of polymer when heated to 850°C. The bigger residue implies the

good fire resistance in the condensed phase flame retarding mechanism.

DTA curves presented in Figure 5 shows the heat effect of untreated and treated LDPE. The order of exothermic amount is LDPE > LDPE/IFR > LDPE/IFR/UZB. The results of TGA and DTA provide the positive evidence that the good synergist effect of UZB on LDPE/IFR existed and this is consistent to the LOI values, especially the results of cone calorimeter test.

#### SEM and EDS

The scanning electron micrograph and energy dispersive spectrograph of residual samples of LDPE/IFR and LDPE/IFR/UZB heated at 550°C for 30 min are illustrated in Figures 6 and 7. "Hills and valleys" to-

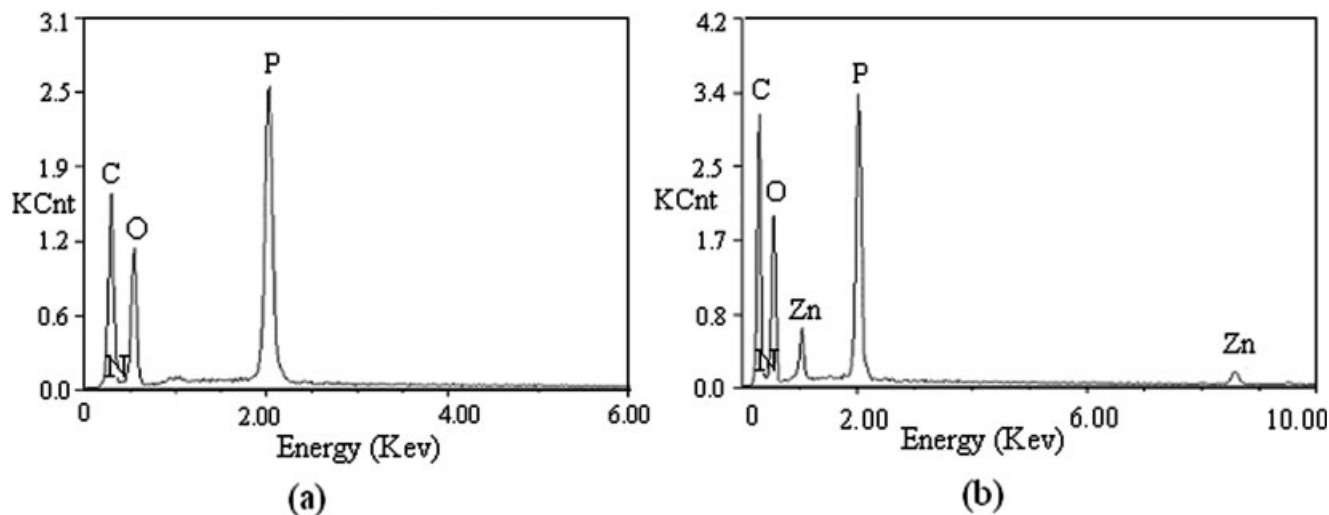


**Figure 7** EDS of residual samples of (a) LDPE/IFR and (b) LDPE/IFR/UZB heated at 550°C for 30 min.

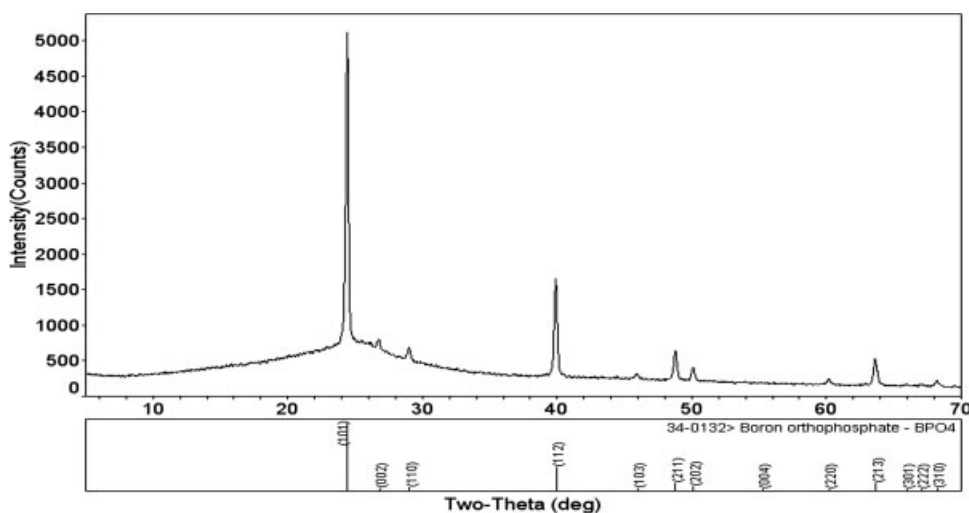


Figure 8 XRD of residual sample of LDPE/IFR/UZB heated at 550°C for 30 min.

pography and “worm” graphite structure can be observed from the scanning electron micrograph of the residual sample of LDPE/IFR/UZB, and cannot be observed from that of the residual sample of LDPE/IFR. The findings of Duquesne et al.<sup>31</sup> illustrated that hills and valleys topography and worm graphite structure favor the fire retardant performance. The scanning electron micrograph provides the positive evidence that the quality of char of LDPE/IFR/UZB is superior to that of LDPE/IFR. The better quality of char plays an important role on the synergist flame retarding effect of UZB on LDPE/IFR. In addition, some little white spots (diameter < 1  $\mu\text{m}$ ) can be seen in the scanning electron micrograph of the former, and this can be attributed to the residual materials of UZB when heated at 550°C. Although the agglomeration occur inevitably at high temperature, the diameter of particle is still smaller than the general zinc borate, which implies that the dispersion of UZB in LDPE/IFR system is good. The results of EDS show that the content of elements in the residual sample of LDPE/IFR/UZB is C (55.97%), N (4.31%), O (25.9%), P (9.55%), Zn (4.32%) and that of LDPE/IFR is C (58.06%), N (2.86%), O (26.41%), P (12.68%). According to the result of XRD, boron existed, but not found in the residual sample of LDPE/IFR/UZB because the elements before carbon cannot be checked out by EDS X-ray microanalysis.

## XRD

XRD of residual sample of LDPE/IFR/UZB is presented in Figure 8. It can be seen that boron orthophosphate ( $\text{BPO}_4$ ) is formed in the residual sample of LDPE/IFR/UZB when heated at 550°C for 30 min. Jimenez et al.<sup>32</sup> found borophosphate when a mixture of boric acid and coated ammonium polyphosphate was treated at 250, 300, and 450°C by solid-state NMR,

and proposed that borates provide the good structural properties of the char owing to the formation of borophosphate because it is a hard material and also shows a good thermal stability. And so, boron orthophosphate may play an important role on improving the char structural properties of LDPE/IFR/UZB, compared with that of LDPE/IFR. Zinc-contained compounds are not found in XRD, although zinc existed according to the results of EDS. It can be explained that the crystallinity of zinc-contained compounds is not good and cannot be detected by XRD, although they exist.

## CONCLUSIONS

The flame retardancy is improved when incorporating UZB to LDPE/IFR system especially UL-94 can reach V0 rating when the mass ratio of UZB to IFR is 4.2 : 25.8 and the content of complex flame retardant is 30% (based on LDPE).

Cone calorimetry experiments give much clearer evidence than did the LOI measurements that incorporation of UZB into LDPE/IFR system resulted in HRR, THR, and mass loss reduce significantly.

TGA results show that the residue of LDPE/IFR/UZB is obviously higher than that of LDPE/IFR when the temperature is above 600°C. The combination of TGA-DTA and SEM indicates that the synergist flame retarding effect of UZB on LDPE/IFR system results from the excellent quality of char that can better endure the oxidation of high temperature and slows the degradation of the LDPE/IFR.

The results of EDS and XRD indicate that boron orthophosphate ( $\text{BPO}_4$ ) and zinc-contained compounds are formed when LDPE/IFR/UZB is heated at 550°C. It may be proposed that boron orthophosphate and zinc-contained compound play an important role on improving the properties of intumescent

char structure of LDPE/IFR/UZB, compared with that of LDPE/IFR. So the degradation speed of LDPE/IFR/UZB is decreased substantially when compared with that of LDPE/IFR when subjected to high temperature.

## References

1. Lin, S.; Wang, X. F.; Wu, Y. P. *Polymer Materials*; China Light Industry Press: Beijing, 2000.
2. Ou, Y. X. *Applied Flame Retarding Technology*; China Chem Industry Press: Beijing, 2002.
3. Fu, H. Q.; Huang, H.; Zhang, X. Y.; Chen, F. Q. *China Syn Resin Plast* 2004, 21, 77.
4. Mauerer, O. *Polym Degrad Stab* 2005, 88, 70.
5. Montaudo, G.; Puglisi, C. *Polym Prepr* 1989, 30, 524.
6. Bourbigot, S.; Duquesne, S.; Leroy, J. M. *J Fire Sci* 1999, 17, 42.
7. Almeras, X.; Le Bras, M.; Hornsby, P.; Bourbigot, S.; Marosi, G.; Keszei, S.; Poutch, F. *Polym Degrad Stab* 2003, 82, 325.
8. Montaudo, G.; Scamporrino, E. *J Appl Polym Sci* 1985, 30, 1449.
9. Bourbigot, S.; Le bras, M.; Delobel, R. *Carbon* 1993, 31, 1219.
10. Li, B.; Xu, M. J. *Polym Degrad Stab* 2006, 91, 1380.
11. Li, B.; Sun, S. Y.; Zhang, X. C. *Chem J Chin Univ* 1999, 20, 146.
12. Xie, F.; Wang, Y. Z.; Yang, B. *Macromol Mater Eng* 2006, 29, 247.
13. Hu, X. P.; Li, Y. L.; Wang, Y. Z. *Macromol Mater Eng* 2004, 289, 208.
14. Giúdice, C. A.; Benítez, J. C. *Prog Organic Coat* 2001, 42, 82.
15. Schubert, D. M.; Calif, L. A. U.S. Pat. 5,472,644 (1995).
16. Bourbigot, S.; Le Bras, M.; Leeuwendal, R.; Shen, K. K.; Schubert, D. *Polym Degrad Stab* 1999, 64, 419.
17. Carpentier, F.; Bourbigot, S.; Le Bras, M.; Delobel, R.; Foulon, M. *Polym Degrad Stab* 2000, 69, 83.
18. Kim, S. *J Polym Sci* 2003, 41, 936.
19. Xie, R. C.; Qu, B. J. *J Appl Polym Sci* 2001, 89, 1181.
20. Bourbigot, S.; Le Bras, M.; Duquesne, S.; Rochery, M. *Macromol Mater Eng* 2004, 289, 499.
21. Le Bras, M.; Bourbigot, S.; Duquesne, S.; Jama, C.; Wilkie, C. A. *Fire Retardancy of Polymers: New Applications of Mineral Fillers*; Royal Society of Chemistry Press: Cambridge, 2005, 327 pp.
22. Dong, J. X.; Hu, Z. S. *Tribol Int* 1998, 31, 219.
23. Diagne, M.; Guèye, M.; Vidal, L.; Tidjani, A. *Polym Degrad Stab* 2005, 89, 418.
24. Wu, Z. P.; Shu, W. Y.; Hu, Y. C.; Xiong, L. M. *China Plast* 2005, 19, 83.
25. Wu, Z. P.; Shu, W. Y.; Hu, Y. C. *China Plast* 2006, 20, 69.
26. Bourbigot, S.; Duquesne, S.; Jama, C. *Macromol Symposia* 2006, 233, 180.
27. Lu, H.; Hu, Y.; Xiao, J. *Mater Lett* 2005, 59, 648.
28. Price, D.; Bullett, K. J.; Cunliffe, L. K.; Hull, T. R.; Milnes, G. J.; Ebdon, J. R.; Hunt, B. J.; Joseph, P. *Polym Degrad Stab* 2005, 88, 74.
29. Redfern, J. *Mater World* 1996, 4, 73.
30. Kandola, B. K.; Horrocks, S.; Horrocks, A. R. *Thermochimica Acta* 1997, 294, 113.
31. Duquesne, S.; Delobel, R.; Le Bras, M.; Camino, G. *Polym Degrad Stab* 2002, 77, 333.
32. Jimenez, M.; Duquesne, S.; Bourbigot, S. *Thermochimica Acta*, to appear.